

SEE-DPO: Self Entropy Enhanced Direct Preference Optimization

Shivanshu Shekhar

University of Illinois Urbana-Champaign

shekhar6@illinois.edu

Shreyas Singh

Indian Institute of Technology, Madras

itsshreyas1803@gmail.com

Tong Zhang

University of Illinois Urbana-Champaign

tozhang@illinois.edu

Abstract

Direct Preference Optimization (DPO) has been successfully used to align large language models (LLMs) according to human preferences, and more recently it has also been applied to improving the quality of text-to-image diffusion models. However, DPO-based methods such as SPO, Diffusion-DPO, and D3PO are highly susceptible to overfitting and reward hacking, especially when the generative model is optimized to fit out-of-distribution during prolonged training. To overcome these challenges and stabilize the training of diffusion models, we introduce a self-entropy regularization mechanism in reinforcement learning from human feedback. This enhancement improves DPO training by encouraging broader exploration and greater robustness. Our regularization technique effectively mitigates reward hacking, leading to improved stability and enhanced image quality across the latent space. Extensive experiments demonstrate that integrating human feedback with self-entropy regularization can significantly boost image diversity and specificity, achieving state-of-the-art results on key image generation metrics.

1. Introduction

Recent advancements in text-to-image generation models have achieved remarkable success [25, 27–29], enabling the creation of high-quality images that are both visually striking and semantically coherent. By leveraging large-scale image datasets, these models have demonstrated an unprecedented ability to generate images that align closely with the intended descriptions. This progress has garnered significant attention, highlighting the vast potential for practical applications in fields such as art, design, and content generation, while also raising important questions regarding the broader implications of such technology. [10, 28, 29]

Text-to-image generation models are typically pre-trained on vast datasets, which often contain low-quality contents, leading to the introduction of various deficiencies in the trained models [27]. To mitigate these issues and improve the quality of generated outputs, additional post-training steps are usually required. Common approaches for post-training include Supervised Fine-Tuning (SFT) [6] and Reinforcement Learning with Human Feedback (RLHF) [9]. RLHF has gained popularity in recent years due to its ability to improve generative model’s ability using self generated data [3]. RLHF has been highly successful in aligning LLMs [7, 24, 26], and more recently it has demonstrated great potential for enhancing the generation quality of diffusion models [4, 11, 22, 34, 39].

Standard RLHF algorithms rely on a reward model to evaluate output images and a learning algorithm, such as Proximal Policy Optimization (PPO) [30] or REINFORCE [41], to adjust the generative model based on these rewards. Reward models are often trained on human preference data [18, 36]. More recently, it was shown that Direct Preference Optimization (DPO) can be used to train large language model directly on preference data without reward modeling. The algorithm became popular because it yields competitive performance and is more stable to train than PPO, and has since been applied to diffusion models as well [22, 34, 39]. Methods like D3PO [39], SPO [22] and Diffusion-DPO [34] adapt the DPO objective to train diffusion models. Some more recent studies showed that for large language models, online iterative DPO, plus reward model learning, is superior to DPO [37, 40], and similar techniques can be applied to diffusion models as well. Online DPO algorithms consist of two key steps: sample generation and model training. At each timestep, the current model undergoes fine-tuning on the available dataset using DPO. Following this, new samples are generated from the updated model. These samples

are subsequently evaluated and ranked by an existing reward model. The newly scored data is then appended to the existing dataset, ensuring continuous improvement and adaptation of the model. This is the approach we will employ in this paper.

However, for large language models, when we use online iterative DPO for multiple iterations, the generation model deteriorates significantly due to significant shifts from the original distribution which leads to artificially high rewards and mode collapse. This phenomenon, referred to as reward hacking [38], is a challenging problem which we have also observed in diffusion models. [Fig: 1]

A commonly used method to mitigate reward hacking is to include an KL regularization term in the objective function that enforces the trained language model to be close to the pretrained model (reference distribution) [9]. We observe that this regularization, while alleviating the reward hacking problem, is insufficient to prevent it for diffusion models. We identify a key reason of this to be that pretrained diffusion model’s generation is not diverse enough, and thus after RLHF, the trained model will have further reduced diversity. To address this problem, we propose to incorporate an additional self-entropy regularization to improve diversity. Mathematically, we demonstrate that this approach flattens the reference distribution in the KL-divergence term. Therefore the regularization condition encourages the model to be more exploratory, effectively reducing overfitting and mitigating reward hacking. We also show that the strength of this regularization requires minimal hyperparameter tuning, maintaining strong performance across a broad range of values. Moreover, our method achieves state-of-the-art performance across various metrics. Finally, we qualitatively show that our approach generates more diverse and aesthetically superior images compared to existing methods, which tend to produce high-quality results only for a limited subset of the input latent space for a given prompt (that is, lacks diversity). Our main contributions are as follows:

1. We introduce a novel self-entropy regularization term into the standard KL-regularized formulation of RLHF objective function. It is shown that this additional term can effectively improve RLHF results for diffusion models.
2. Our method is effective in mitigating reward hacking in DPO-based algorithms for diffusion models. When combined with the prior state-of-the-art method D3PO, Diffusion-DPO and SPO we are able to obtain new state-of-the-art results on various image quality metrics.
3. We carry out empirical studies to demonstrate that this regularization technique encourages broader exploration of the solution space, reducing overfitting and preventing reward hacking. Moreover, we achieve enhanced stability and image quality across the latent space of the diffu-

sion model, leading to more consistent outputs.

2. Related Works

Diffusion Model: Diffusion models have become state-of-the-art in image generation [25, 27], with methods like Denoising Diffusion Probabilistic Models (DDPM) [15] and Denoising Diffusion Implicit Models (DDIM) [31] significantly improving both image quality and generation speed. Text-to-image diffusion models, in particular, have enabled the creation of highly detailed and realistic digital art [25, 27, 28]. Increasing interest has focused on adapting these models to specialized domains [1, 8, 16, 21], such as chemical structure generation [29], where tuning the full model is computationally expensive.

Works like [17, 19, 23] have introduced methods such as adapters and compositional approaches to combine multiple models, enhancing specificity, control, and output quality while lowering the computational needs for training. Additionally, classifier-free guidance (CFG) [14] has streamlined the sampling process by removing the need for a separate classifier, instead relying on the model’s predictions of both conditional and unconditional noise to improve quality and diversity. In contrast, classifier-based guidance [10], while providing more precise control, comes with higher computational costs due to the need for an external classifier.

RLHF: RLHF [9] has become a pivotal technique for aligning the outputs of foundational models with human preferences by incorporating human feedback during the training process. This method enables models to be fine-tuned to generate behaviorally aligned outputs, addressing issues like bias or harmful content. RLHF has been successfully applied across diverse domains, from developing policies for Atari games to training robotic systems [3].

Notably, OpenAI’s GPT series [24] has showcased the impact of RLHF in enhancing language model performance, other parallel works have also shown a similar improvement across tasks [2, 12, 33], particularly in improving coherence, relevance, and user experience. In parallel, Reinforcement Learning from AI Feedback (RLAIF) has been proposed as a cost-effective alternative, utilizing AI systems for feedback to scale model refinement. In this paper, we adopt RLAIF to generate high-quality images and achieve state-of-the-art performance across multiple evaluation metrics.

DPO: A key challenge in RLHF lies in designing an effective reward function, which typically requires a large, curated dataset for training in order to achieve competitive

results [9]. Even after constructing the reward model, it is vulnerable to manipulation by policies, especially for out-of-distribution (OOD) samples, leading to artificially inflated rewards. Additionally, training the main policy while simultaneously loading the reward model into memory introduces further computational complexity.

To address these issues, [26] introduced Direct Preference Optimization (DPO), a method that fine-tunes language models directly from user preferences, leveraging the correlation between reward functions and optimal policies. However, this approach does not directly extend to diffusion models, as DPO operates within the Contextual Bandit framework, which treats generation as a single-step process, whereas diffusion models require handling latent states over multiple timesteps, making storage infeasible even with techniques like LoRA [17]. Diffusion-DPO [34] adapts this by optimizing an upper bound on the true loss function, D3PO [39] models the diffusion process as a Markov Decision Process (MDP), using the action-value function instead of a traditional reward model at each generation step. This approach assumes that the chain generating the preferred response is best at every step. In contrast, SPO [22] introduces training a reward model that can score samples across varying noise levels, allowing for effective optimization of the DPO objective throughout the diffusion process. This method relaxes the strict assumptions made by D3PO, providing a more flexible approach to diffusion modeling.

3. Background

Diffusion Models: Diffusion models are generative models that learn to represent the data distribution $p(\mathbf{x}_0)$ by gradually corrupting data with noise in a forward diffusion process, and subsequently learning to reverse this process. Denoising diffusion models parameterize the data distribution as $p_\theta(\mathbf{x}_0)$, where the reverse process is modeled as a Markov chain. This reverse process is discrete in time and follows the structure:

$$p_\theta(\mathbf{x}_{0:T}) = p(x_T) \prod_{t=1}^T p_\theta(\mathbf{x}_{t-1} | \mathbf{x}_t) \quad (1)$$

where

$$p_\theta(x_{t-1} | x_t) = \mathcal{N}\left(x_{t-1}; \mu_\theta(x_t), \sigma_{t|t-1}^2 \frac{\sigma_{t-1}^2}{\sigma_t^2} \mathbf{I}\right)$$

$$p_T = \mathcal{N}(x_T; 0, \mathbf{I})$$

The model is trained by maximizing the evidence lower bound (ELBO) on the data likelihood. The training objective for diffusion models is defined as:

$$L_{DM} = \mathbb{E}_{\mathbf{x}_0, \epsilon, t, \mathbf{x}_t} [\omega(\lambda_t) \|\epsilon - \epsilon_\theta(\mathbf{x}_t, t)\|_2^2] \quad (2)$$

Here, the noise ϵ is sampled from a normal distribution, i.e., $\epsilon \sim \mathcal{N}(\mu, \mathbf{I})$, and the time step t is sampled uniformly from the range $t \sim \mathcal{U}(0, T)$. The corrupted image \mathbf{x}_t is sampled from a Gaussian distribution conditioned on the original image, $q(\mathbf{x}_t | \mathbf{x}_0) = \mathcal{N}(\mathbf{x}_t; \alpha_t \mathbf{x}_0, \sigma_t^2 \mathbf{I})$, where $\lambda_t = \alpha_t^2 / \sigma_t^2$ represents the signal-to-noise ratio. The function $\omega(\lambda_t)$ is a predefined weighting function, often chosen as a constant for simplicity.

Reward Modelling: Reward modeling focuses on modeling human preferences for a generated sample \mathbf{x} under a specific conditioning c . To achieve this a human-annotated dataset is usually used which usually contain triplets $(\mathbf{x}_w, \mathbf{x}_l, c)$, where \mathbf{x}_w represents the preferred (winning) sample and \mathbf{x}_l represents the less preferred (losing) sample given the conditioning c .

For preference learning which is used in online iterative DPO, usually the Bradley-Terry (BT) model is used [5] to describe the probability that \mathbf{x}_w is preferred over \mathbf{x}_l conditioned on c , which is formalized as:

$$p_{BT}(\mathbf{x}_w \succ \mathbf{x}_l | c) = \sigma(r(c, \mathbf{x}_w) - r(c, \mathbf{x}_l)) \quad (3)$$

where $r(c, x)$ denotes the reward function.

The reward function is parametrized as $r_\phi(c, x)$, where ϕ represents the model parameters, and we finally optimize the log-likelihood of Eq. (3) as the primary learning objective:

$$L_{BT}(\phi) = -\mathbb{E}_{c, \mathbf{x}_w, \mathbf{x}_l} [\log \sigma(r_\phi(c, \mathbf{x}_w) - r_\phi(c, \mathbf{x}_l))] \quad (4)$$

DPO: Reinforcement Learning from Human Feedback (RLHF) aims to optimize a conditional distribution $p_\theta(\mathbf{x}_0 | c)$ over latents \mathbf{x}_0 conditioned on context c . The objective of RLHF is commonly framed as maximizing the expected reward while minimizing divergence from a reference policy. Mathematically, the objective can be expressed as:

$$\max_{p_\theta} \mathbb{E}_{c \sim \mathcal{D}_c, x_0 \sim p_\theta(x_0 | c)} [r(c, x_0)] - \beta \mathcal{D}_{KL} [p_\theta(x_0 | c) \| p_{\text{ref}}(x_0 | c)] \quad (5)$$

In Eq. (5), the first term encourages the policy to maximize the expected reward, while the second term, weighted by a hyperparameter β , introduces a regularization to keep the current policy close to a reference policy p_{ref} . In this formulation, β controls the trade-off between exploration (reward maximization) and exploitation (closeness to the reference policy).

However, this formulation assumes that the reward model is ideal, which is often not the case in practice. Training and querying a reward model typically incurs high computational costs, making the approach challenging to scale.



Figure 1. **Effect of Entropy Regularization on reward hacking.** Figure 1 demonstrates the effectiveness of entropy regularization for mitigating reward hacking problems during Direct Preference Optimization (DPO) [38]

To address this issue, Direct Policy Optimization (DPO) reformulates the problem to directly solve for the optimal policy p_θ^* in a closed form, defined as:

$$p_\theta^*(\mathbf{x}_0|c) = p_{\text{ref}}(\mathbf{x}_0|c) \exp\left(\frac{r(c, \mathbf{x}_0)}{\beta}\right) / Z(c) \quad (6)$$

Here, $Z(c)$ is the partition function:

$$Z(c) = \sum_{x_0} p_{\text{ref}}(x_0|c) \exp\left(\frac{r(c, x_0)}{\beta}\right) \quad (7)$$

This leads to a rewritten form of the reward function:

$$r(c, x_0) = \beta \log \frac{p_\theta^*(x_0|c)}{p_{\text{ref}}(x_0|c)} + \beta \log Z(c) \quad (8)$$

Substituting this into the original objective in Eq. (8), the reward objective for DPO becomes:

$$L_{\text{DPO}}(\theta) = -\mathbb{E}_{c, x_0^w, x_0^l} \left[\log \sigma \left(\beta \log \frac{p_\theta(x_0^w|c)}{p_{\text{ref}}(x_0^w|c)} - \beta \log \frac{p_\theta(x_0^l|c)}{p_{\text{ref}}(x_0^l|c)} \right) \right] \quad (9)$$

This reparameterization allows DPO to bypass the need for reward function optimization and instead directly optimizes the conditional distribution $p_\theta(x_0|c)$. All DPO-based

diffusion methods Diffusion-DPO, D3PO & SPO introduce approximation techniques to apply this approach to diffusion models. In this paper, we show that all these approaches are mathematically similar and we further introduce our self-entropy regularization in this unified framework.

4. Methodology

In this section, we prove the equivalence of D3PO, SPO, and DiffusionDPO. We model the diffusion process as an MDP, we use the notations from [39]:

$$\begin{aligned} s_t &\triangleq (c, t, x_{T-t}) \\ P(s_{t+1} | s_t, a_t) &\triangleq (\delta_c, \delta_{t+1}, \delta x_{T-1-t}) \\ a_t &\triangleq x_{T-1-t} \\ \pi(a_t | s_t) &\triangleq p_\theta(x_{T-1-t} | c, t, x_{T-t}) \\ r(s_t, a_t) &\triangleq r((c, t, x_{T-t}), x_{T-t-1}) \end{aligned}$$

Where T is the maximum number of denoising timesteps and δ_x represents a Dirac delta distribution. We want to

optimize Eq. (9), we can re-write it as:

$$L_{\text{DPO}}(\theta) = -\mathbb{E}_{c, x_0^w, x_0^b} \left[\log \sigma \left(\beta \log \prod_i \frac{p_\theta(x_{t-1}^w | x_t^w)}{p_{\text{ref}}(x_{t-1}^w | x_t^w)} - \beta \log \prod_i \frac{p_\theta(x_{t-1}^l | x_t^l)}{p_{\text{ref}}(x_{t-1}^l | x_t^l)} \right) \right] \quad (10)$$

We don't write the conditioning on c explicitly in Eq. (10) for conciseness. This can be further written as:

$$L_{\text{DPO}}(\theta) = -\mathbb{E}_{c, x_0^w, x_0^b} \left[\log \sigma \left(\beta \sum_{t=1}^N \log \frac{p_\theta(x_{t-1}^w | x_t^w)}{p_{\text{ref}}(x_{t-1}^w | x_t^w)} - \beta \sum_{t=1}^M \log \frac{p_\theta(x_{t-1}^l | x_t^l)}{p_{\text{ref}}(x_{t-1}^l | x_t^l)} \right) \right] \quad (11)$$

Where N, M are the number of timesteps in the winning and losing sample generation respectively.

We assume that $N = M = T$, and using [39], we can further write the objective as:

$$L_{\text{DPO}}(\theta) = -\mathbb{E}_{c, x_0^w, x_0^b} \left[\log \sigma \left(\beta T * \frac{1}{T} * \sum_{t=1}^T \log \frac{p_\theta(x_{t-1}^w | x_t^w)}{p_{\text{ref}}(x_{t-1}^w | x_t^w)} - \beta T * \frac{1}{T} * \sum_{t=0}^T \log \frac{p_\theta(x_{t-1}^l | x_t^l)}{p_{\text{ref}}(x_{t-1}^l | x_t^l)} \right) \right] \quad (12)$$

We can define t as a random variable which is sample from a uniform distribution with support from 0 to T . Using this and Jensen Shannon inequality we arrive at:

$$L_{\text{DPO}}(\theta) = -\mathbb{E}_{c, x_0^w, x_0^b} \left[\log \sigma \left(\beta T * \mathbb{E}_{t \sim \mathcal{U}(0, T)} \left[\log \frac{p_\theta(x_{t-1}^w | x_t^w)}{p_{\text{ref}}(x_{t-1}^w | x_t^w)} - \log \frac{p_\theta(x_{t-1}^l | x_t^l)}{p_{\text{ref}}(x_{t-1}^l | x_t^l)} \right] \right) \right] \quad (13)$$

$$L_{\text{DPO}}(\theta) \leq -\mathbb{E}_{c, x_0^w, x_0^b, t \sim \mathcal{U}(0, T)} \left[\log \sigma \left(\beta T \log \frac{p_\theta(x_{t-1}^w | x_t^w)}{p_{\text{ref}}(x_{t-1}^w | x_t^w)} - \beta T \log \frac{p_\theta(x_{t-1}^l | x_t^l)}{p_{\text{ref}}(x_{t-1}^l | x_t^l)} \right) \right] \quad (14)$$

This objective is similar to Diffusion-DPO, if instead we consider optimization at each step then the objective translates to SPO and D3PO's objective.

Now we introduce our self-entropy regularization into this framework. We start with D3PO's formulation:

$$\max_{\pi} \mathbb{E}_{s \sim d^{\pi}, a \sim \pi(\cdot | s)} [Q^*(s, a)] - \beta \left(D_{\text{KL}} [\pi(a|s) \| \pi_{\text{ref}}(a|s)] + \gamma \pi(a|s) \log \frac{\pi(a|s)}{\pi_{\text{ref}}(a|s)} \right) \quad (15)$$

Given the objective of Eq. (15), the action-value function can be written in term of the optimal policy $\pi^*(a|s)$ as:

$$Q^*(s, a) = \beta \left(\log \frac{\pi^*(a|s)}{\pi_{\text{ref}}(a|s)} + \gamma \log \pi^*(a|s) \right) \quad (16)$$

Plugging Eq. (16) in the Bardley-Terry Model and optimizing the log-likelihood we get the following objective function:

$$\mathcal{L}(\theta) = -\mathbb{E}_{(s_k, \sigma_w, \sigma_l)} \left[\log \rho \left(\beta(\gamma + 1) \cdot \left(\log \frac{\pi_\theta(a_k^w | s_k^w)}{\pi_{\text{ref}}(a_k^w | s_k^w)^{\frac{1}{\gamma+1}}} - \log \frac{\pi_\theta(a_k^l | s_k^l)}{\pi_{\text{ref}}(a_k^l | s_k^l)^{\frac{1}{\gamma+1}}} \right) \right) \right] \quad (17)$$

From Eq. (17) we can see that the final effect of adding the self-entropy term was to flatten out the reference distribution which in return forces the policy to be more explorative. We can also write this in terms of the noise objective similar to Diffusion-DPO:

$$L_w = (1 + \gamma) \left(\|\epsilon^w - \epsilon_\theta(x_t^w, t)\|^2 - \|\epsilon^l - \epsilon_\theta(x_t^l, t)\|^2 \right) \\ L_l = \left(\|\epsilon^w - \epsilon_{\text{ref}}(x_t^w, t)\|^2 - \|\epsilon^l - \epsilon_{\text{ref}}(x_t^l, t)\|^2 \right) \\ L_{\text{final}}(\theta) \leq -\mathbb{E}_{t, \epsilon^w, \epsilon^l} \log \sigma \left(-\beta T (L_w - L_l) \right).$$

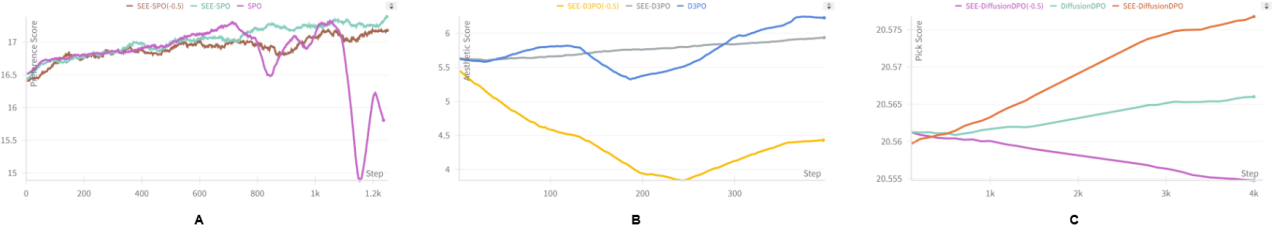


Figure 2. **Accuracy vs Steps** A: Step-Wise PickScore [22], B: Aesthetic Score[35], C: Pick Score [18], demonstrate faster convergence, improved training stability and robustness to reward hacking.

Method	PickScore \uparrow	HPS \uparrow	Aesthetic Score \uparrow	BLIP \uparrow	ImageReward \uparrow	CLIP \uparrow
DPOK	20.583	0.260	4.705	0.498	0.099	0.270
DDPO	20.569	0.260	4.683	0.498	0.090	0.270
D3PO	20.306	0.227	5.050	0.470	-0.209	0.261
DiffusionDPO	20.791	0.262	4.711	0.486	0.139	0.263
SPO	20.919	0.266	4.702	0.472	0.191	0.249
SEE-D3PO	20.590	0.247	4.851	0.491	-0.003	0.271
SEE-DiffusionDPO	20.854	0.270	4.714	0.491	0.225	0.265
SEE-SPO	21.256	0.283	4.673	0.509	0.590	0.273

Table 1. All numbers are reported on the validation-unique split of Pick-a-Pic V1 dataset. We evaluate on CLIP Score [13], BLIP Score [20], Aesthetic Score [35], Pick Score [18], HPSv2 Score [36]

We could start from the formulation of Diffusion-DPO to get an alternate version of our objective which is different only by a constant, we start by optimizing the below objective:

$$\max_{p_\theta} \mathbb{E}_{c \sim \mathcal{D}_c, x_{0:T} \sim p_\theta(x_{0:T}|c)} [r(c, x_0) - \beta \mathbb{D}_{\text{KL}}[p_\theta(x_{0:T}|c) \parallel p_{\text{ref}}(x_{0:T}|c)]] \quad (18)$$

Further let $r(c, x_0) = \mathbb{E}_{p_\theta(x_{1:T}|x_0, c)} [R(c, x_{0:T})]$, plugging this to Eq. (18), upper-bounding KL-divergence and using Jensen’s inequality we get:

Finally, we get our objective:

$$L_w = \omega(\lambda_t) \left(\|\epsilon^w - \epsilon_\theta(x_t^w, t)\|^2 - \|\epsilon^l - \epsilon_\theta(x_t^l, t)\|^2 \right)$$

$$L_l = \omega(\lambda_t(1 + \gamma)) \left(\|\epsilon^w - \epsilon_{\text{ref}}(x_t^w, t)\|^2 - \|\epsilon^l - \epsilon_{\text{ref}}(x_t^l, t)\|^2 \right)$$

$$L_{\text{final}}(\theta) \leq -\mathbb{E}_{t, \epsilon^w, \epsilon^l} \log \sigma \left(-\beta T(L_w - L_l) \right)$$

Further $\omega(t) \propto 1/\sigma_t^2$, in most work [15, 31, 34] $\omega(t)$ is taken a constant. Combining both we write our final objective as:

$$L_w = \left(\|\epsilon^w - \epsilon_\theta(x_t^w, t)\|^2 - \|\epsilon^l - \epsilon_\theta(x_t^l, t)\|^2 \right)$$

$$L_l = \frac{1}{(1 + \gamma)} \left(\|\epsilon^w - \epsilon_{\text{ref}}(x_t^w, t)\|^2 - \|\epsilon^l - \epsilon_{\text{ref}}(x_t^l, t)\|^2 \right)$$

$$L_{\text{final}}(\theta) \leq -\mathbb{E}_{t, \epsilon^w, \epsilon^l} \log \sigma \left(-\beta T(L_w - L_l) \right).$$

We can see that to a constant factor this is similar to one derived Eq. (17). Intuitively, in this formulation, the loss associated with the reference model is reduced when $\gamma > 0$. Therefore the resulting diffusion model relies less on the reference model. This allows the trained model to explore space in which the reference model may not be able to cover, and thus increases the diversity of the trained model.

5. Experiments & Results

We trained the SPO, Diffusion-DPO, and D3PO models using our proposed regularized loss function, applying the default hyperparameters from their respective original implementations. For training, we used prompts from the Pick-a-Pic-V1 dataset for SPO and Diffusion-DPO, and 1,000 ImageReward prompts for D3PO as provided on GitHub, following the same setup and data splits as in the original implementations. For feedback mechanisms, we used PickScore as a stand-in for human feedback in SPO, human annotations from the Pick-a-Pic-V1 dataset for Diffusion-DPO, and the Aesthetic Score for D3PO. The optimal values for β and γ are shown in Table 3. Notably, the optimal β for Diffusion-DPO is two orders of magnitude larger than that of D3PO, which is expected since the β for Diffusion-DPO is multiplied by T , a term of order 2. In the case of

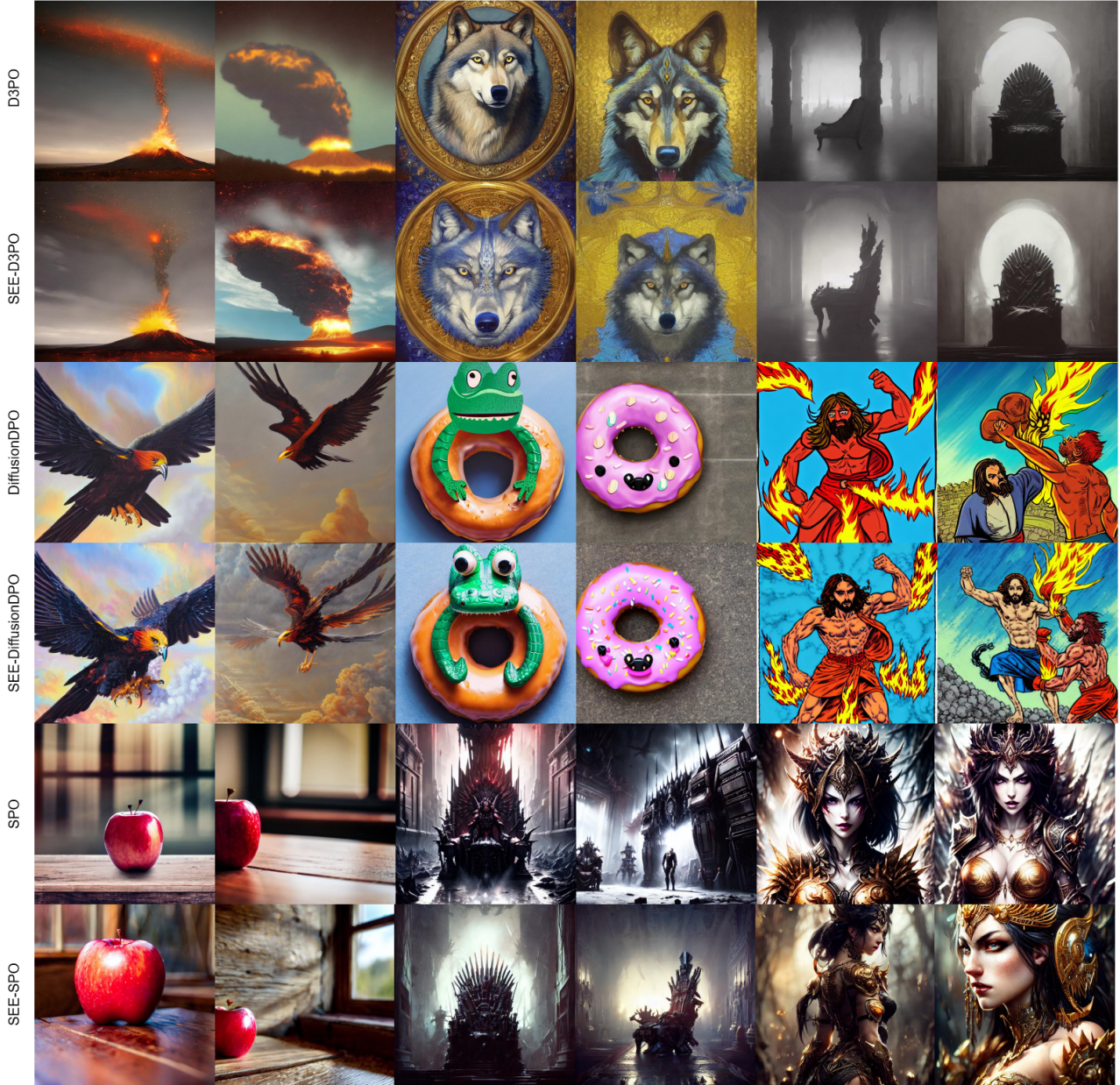


Figure 3. **Enhancing Generation Diversity.** Our method demonstrates superior image quality, producing clearer and more detailed results across different latent variables. In contrast, existing approaches show significant degradation in image quality, with blurring and distortions becoming evident as latent variations increase.

SPO, we update at each timestep, which is of order 1, so we also expect β to increase by one order to prevent significant deviation from the reference distribution.

For our evaluation, we used the validation unique split of the Pick-a-Pic-V1 dataset across all models. We utilized the publicly available models for SPO and Diffusion-DPO, while for D3PO, we trained the model with default param-

eters and used it for evaluation. Table 1 presents the results, showing that our methods outperform previous approaches on most metrics. Notably, SEE-SPO improved HPS score, ImageReward, and PickScore by 6.4%, 166.5%, and 1.62%, respectively, over SPO. Similar performance gains are observed for D3PO and DiffusionDPO as well.

To evaluate the diversity and quality of generated im-

Method	RMSE \uparrow	PSNR \downarrow	SSIM \downarrow	E1 \uparrow	E2 \uparrow
StableDiffusion-1.5	0.3745	8.6943	0.2100	7.4627	7.4620
DiffusionDPO	0.3736	8.7047	0.2406	7.4954	7.4945
SEE-DiffusionDPO	0.3799	8.5324	0.2014	7.5846	7.5836
D3PO	0.2455	12.5599	0.4190	7.0853	7.0911
SEE-D3PO	0.3052	10.5240	0.3183	7.3650	7.3692
SPO	0.4446	7.1218	0.1666	7.5674	7.5635
SEE-SPO	0.3983	8.0818	0.1611	7.7080	7.7047

Table 2. All values are reported on the validation-unique split of the dataset. Evaluation metrics include RMSE, PSNR, SSIM, and energy scores (E1 and E2). E1 combines E1.1 and E1.2, and E2 is the average of E2.1 and E1.2.

Model	γ	β
D3PO	5	0.01
Diffusion-DPO	3.1	3.8
SPO	5	0.5

Table 3. **Hyperparameter values:** All the other hyperparameters values were fixed to the original implementation

ages, we sampled 10 images for each prompt in the validation set and calculated metrics including RMSE, PSNR, 1D-Entropy, 2D-Entropy, and SSIM to measure generation diversity [32]. We did not rely on embedding-based similarity, as images generated from the same prompt, though visually different, tend to cluster closely in embedding space. An effectively aligned model should produce diverse images while maintaining high reward scores. Our results indicate that the regularized versions of D3PO, SPO, and DiffusionDPO achieve higher mean rewards across multiple metrics with improved diversity scores, highlighting enhanced performance in both diversity and image quality compared to baseline methods. Detailed results are provided in Table 2.

Ablations

In our experiments, we explored the effect of different values of γ on both training stability and overall model performance. As shown in Fig. 2, when $\gamma = 0$, representing the baseline or vanilla model, we observe an initial steep drop in reward values, followed by a sudden and rapid increase during both SPO and D3PO training phases. This pattern signals that the model begins to overfit prematurely, leading to the generation of repetitive and noisy images—a phenomenon we define as “reward hacking.” In this scenario, the model exploits reward dynamics by producing images that maximize rewards in the short term but lack diversity and generalizability. Interestingly, this trend is absent in the DiffusionDPO setup, which leverages the extensive Pick-a-Pic-V1 dataset containing over 800,000 images, likely providing more comprehensive training data that mitigates early overfitting. Across all configurations, our model achieves higher scores faster, with more consis-

tent stability in training and fewer abrupt changes in reward values.

As training progresses, our model not only stabilizes but also consistently reaches a higher reward range. We attribute this improvement to the implicit flattening of the reference distribution that higher γ values introduce. This flattening effect broadens the policy distribution, fostering more exploratory behavior and decreasing the likelihood of overfitting to repetitive patterns.

To examine the effects of negative γ values, we set γ to a negative constant and observe empirically poorer results compared to the base model, as shown in Fig. 3. D3PO demonstrates early overfitting tendencies, resulting in sharp reward increases followed by rapid declines. Meanwhile, Diffusion-DPO consistently underperforms relative to other models, as the negative γ value restricts exploratory actions, yielding repetitive outputs that fail to capture meaningful image variations. In the SPO pipeline, overfitting occurs somewhat later than in the vanilla model. This difference can be attributed to SPO’s update policy, which only adjusts the model when it generates images with reward differences that exceed a predetermined threshold. With a negative γ , the generation distribution narrows, limiting the diversity of generated images and, consequently, the frequency of model updates. Further evidence of these observations can be seen by examining the rewards vs. steps graph for SPO $\gamma = -0.5$, where the reward values remain nearly constant throughout most of the training duration before ultimately showing signs of overfitting. This steady reward trend reinforces the observation that the model fails to explore diverse solutions, hindering its ability to generalize and adapt, particularly under negative γ settings.

6. Conclusion

In this paper, we introduced Self-Entropy Enhanced Direct Preference Optimization (SEE-DPO) for fine-tuning diffusion models. We showed existing approaches that optimize Eq. (5) often suffer from overfitting and distribution shift issues. To address these challenges, we introduced a self-entropy regularization term into the objective function, transforming it into the final optimization objec-

tive outlined in Eq. (17). Our empirical results demonstrate that the proposed SEE-DPO, SEE-DiffusionDPO, and SEE-DPO method significantly outperforms their respective counterparts, effectively mitigating the reward hacking problem commonly associated with RLHF approaches and resulting in robust training. Additionally, our method ensures diversity of image generation across the latent space, highlighting its robustness and effectiveness in maintaining high-quality outputs.

References

- [1] Anurag Ajay, Yilun Du, Abhi Gupta, Joshua Tenenbaum, Tommi Jaakkola, and Pulkit Agrawal. Is conditional generative modeling all you need for decision-making?, 2023. 2
- [2] Anthropic. Claude: An ai assistant. <https://www.anthropic.com>, 2024. 2
- [3] Yuntao Bai, Saurav Kadavath, Sandipan Kundu, Amanda Askell, Jackson Kernion, Andy Jones, Anna Chen, Anna Goldie, Azalia Mirhoseini, Cameron McKinnon, Carol Chen, Catherine Olsson, Christopher Olah, Danny Hernandez, Dawn Drain, Deep Ganguli, Dustin Li, Eli Tran-Johnson, Ethan Perez, Jamie Kerr, Jared Mueller, Jeffrey Ladish, Joshua Landau, Kamal Ndousse, Kamile Lukosuite, Liane Lovitt, Michael Sellitto, Nelson Elhage, Nicholas Schiefer, Noemi Mercado, Nova DasSarma, Robert Lasenby, Robin Larson, Sam Ringer, Scott Johnston, Shauna Kravec, Sheer El Showk, Stanislav Fort, Tamera Lanham, Timothy Telleen-Lawton, Tom Conerly, Tom Henighan, Tristan Hume, Samuel R. Bowman, Zac Hatfield-Dodds, Ben Mann, Dario Amodei, Nicholas Joseph, Sam McCandlish, Tom Brown, and Jared Kaplan. Constitutional ai: Harmlessness from ai feedback, 2022. 1, 2
- [4] Kevin Black, Michael Janner, Yilun Du, Ilya Kostrikov, and Sergey Levine. Training diffusion models with reinforcement learning, 2024. 1
- [5] Ralph Allan Bradley and Milton E Terry. Rank analysis of incomplete block designs: I. the method of paired comparisons. *Biometrika*, 39(3/4):324–345, 1952. 3
- [6] Tom B. Brown, Benjamin Mann, Nick Ryder, Melanie Subbiah, Jared Kaplan, Prafulla Dhariwal, Arvind Neelakantan, Pranav Shyam, Girish Sastry, Amanda Askell, Sandhini Agarwal, Ariel Herbert-Voss, Gretchen Krueger, Tom Henighan, Rewon Child, Aditya Ramesh, Daniel M. Ziegler, Jeffrey Wu, Clemens Winter, Christopher Hesse, Mark Chen, Eric Sigler, Mateusz Litwin, Scott Gray, Benjamin Chess, Jack Clark, Christopher Berner, Sam McCandlish, Alec Radford, Ilya Sutskever, and Dario Amodei. Language models are few-shot learners, 2020. 1
- [7] Tom B. Brown, Benjamin Mann, Nick Ryder, Melanie Subbiah, Jared Kaplan, Prafulla Dhariwal, Arvind Neelakantan, Pranav Shyam, Girish Sastry, Amanda Askell, Sandhini Agarwal, Ariel Herbert-Voss, Gretchen Krueger, Tom Henighan, Rewon Child, Aditya Ramesh, Daniel M. Ziegler, Jeffrey Wu, Clemens Winter, Christopher Hesse, Mark Chen, Eric Sigler, Mateusz Litwin, Scott Gray, Benjamin Chess, Jack Clark, Christopher Berner, Sam McCandlish, Alec Radford, Ilya Sutskever, and Dario Amodei. Language models are few-shot learners, 2020. 1
- [8] Cheng Chi, Zhenjia Xu, Siyuan Feng, Eric Cousineau, Yilun Du, Benjamin Burchfiel, Russ Tedrake, and Shuran Song. Diffusion policy: Visuomotor policy learning via action diffusion, 2024. 2
- [9] Paul Christiano, Jan Leike, Tom B. Brown, Miljan Martic, Shane Legg, and Dario Amodei. Deep reinforcement learning from human preferences, 2023. 1, 2, 3
- [10] Prafulla Dhariwal and Alex Nichol. Diffusion models beat gans on image synthesis, 2021. 1, 2
- [11] Ying Fan, Olivia Watkins, Yuqing Du, Hao Liu, Moonkyung Ryu, Craig Boutilier, Pieter Abbeel, Mohammad Ghavamzadeh, Kangwook Lee, and Kimin Lee. Dpok: Reinforcement learning for fine-tuning text-to-image diffusion models, 2023. 1
- [12] Google. Google bard: An ai language model. <https://bard.google.com>, 2024. 2
- [13] Jack Hessel, Ari Holtzman, Maxwell Forbes, Ronan Le Bras, and Yejin Choi. Clipscore: A reference-free evaluation metric for image captioning, 2022. 6
- [14] Jonathan Ho and Tim Salimans. Classifier-free diffusion guidance, 2022. 2
- [15] Jonathan Ho, Ajay Jain, and Pieter Abbeel. Denoising diffusion probabilistic models, 2020. 2, 6
- [16] Jonathan Ho, William Chan, Chitwan Saharia, Jay Whang, Ruiqi Gao, Alexey Gritsenko, Diederik P. Kingma, Ben Poole, Mohammad Norouzi, David J. Fleet, and Tim Salimans. Imagen video: High definition video generation with diffusion models, 2022. 2
- [17] Edward J. Hu, Yelong Shen, Phillip Wallis, Zeyuan Allen-Zhu, Yuanzhi Li, Shean Wang, Lu Wang, and Weizhu Chen. Lora: Low-rank adaptation of large language models, 2021. 2, 3
- [18] Yuval Kirstain, Adam Polyak, Uriel Singer, Shahbuland Matiana, Joe Penna, and Omer Levy. Pick-a-pic: An open dataset of user preferences for text-to-image generation, 2023. 1, 6
- [19] Xin Lai, Zhuotao Tian, Yukang Chen, Yanwei Li, Yuhui Yuan, Shu Liu, and Jiaya Jia. Lisa: Reasoning segmentation via large language model, 2024. 2
- [20] Junnan Li, Dongxu Li, Caiming Xiong, and Steven Hoi. Blip: Bootstrapping language-image pre-training for unified vision-language understanding and generation, 2022. 6
- [21] Ronghui Li, Junfan Zhao, Yachao Zhang, Mingyang Su, Zeping Ren, Han Zhang, Yansong Tang, and Xiu Li. Finedance: A fine-grained choreography dataset for 3d full body dance generation, 2023. 2
- [22] Zhanhao Liang, Yuhui Yuan, Shuyang Gu, Bohan Chen, Tiankai Hang, Ji Li, and Liang Zheng. Step-aware preference optimization: Aligning preference with denoising performance at each step, 2024. 1, 3, 6
- [23] Tongxu Luo, Jiahe Lei, Fangyu Lei, Weihao Liu, Shizhu He, Jun Zhao, and Kang Liu. Moelora: Contrastive learning guided mixture of experts on parameter-efficient fine-tuning for large language models, 2024. 2

- [24] OpenAI, Josh Achiam, Steven Adler, Sandhini Agarwal, Lama Ahmad, Ilge Akkaya, Florencia Leoni Aleman, Diogo Almeida, Janko Altenschmidt, Sam Altman, Shyamal Anadkat, Red Avila, Igor Babuschkin, Suchir Balaji, Valerie Balcom, Paul Baltescu, Haiming Bao, Mohammad Bavarian, Jeff Belgum, Irwan Bello, Jake Berdine, Gabriel Bernadett-Shapiro, Christopher Berner, Lenny Bogdonoff, Oleg Boiko, Madelaine Boyd, Anna-Luisa Brakman, Greg Brockman, Tim Brooks, Miles Brundage, Kevin Button, Trevor Cai, Rosie Campbell, Andrew Cann, Brittany Carey, Chelsea Carlson, Rory Carmichael, Brooke Chan, Che Chang, Fotis Chantzis, Derek Chen, Sully Chen, Ruby Chen, Jason Chen, Mark Chen, Ben Chess, Chester Cho, Casey Chu, Hyung Won Chung, Dave Cummings, Jeremiah Currier, Yunxing Dai, Cory Decareaux, Thomas Degry, Noah Deutsch, Damien Deville, Arka Dhar, David Dohan, Steve Dowling, Sheila Dunning, Adrien Ecoffet, Atty Eleti, Tyna Eloundou, David Farhi, Liam Fedus, Niko Felix, Simón Posada Fishman, Juston Forte, Isabella Fulford, Leo Gao, Elie Georges, Christian Gibson, Vik Goel, Tarun Gogineni, Gabriel Goh, Rapha Gontijo-Lopes, Jonathan Gordon, Morgan Grafstein, Scott Gray, Ryan Greene, Joshua Gross, Shixiang Shane Gu, Yufei Guo, Chris Hallacy, Jesse Han, Jeff Harris, Yuchen He, Mike Heaton, Johannes Heidecke, Chris Hesse, Alan Hickey, Wade Hickey, Peter Hoeschele, Brandon Houghton, Kenny Hsu, Shengli Hu, Xin Hu, Joost Huizinga, Shantanu Jain, Shawn Jain, Joanne Jang, Angela Jiang, Roger Jiang, Haozhun Jin, Denny Jin, Shino Jomoto, Billie Jonn, Heewoo Jun, Tomer Kaftan, Łukasz Kaiser, Ali Kamali, Ingmar Kanitscheider, Nitish Shirish Keskar, Tabarak Khan, Logan Kilpatrick, Jong Wook Kim, Christina Kim, Yongjik Kim, Jan Hendrik Kirchner, Jamie Kiros, Matt Knight, Daniel Kokotajlo, Łukasz Kondraciuk, Andrew Kondrich, Aris Konstantinidis, Kyle Kosic, Gretchen Krueger, Vishal Kuo, Michael Lampe, Ikai Lan, Teddy Lee, Jan Leike, Jade Leung, Daniel Levy, Chak Ming Li, Rachel Lim, Molly Lin, Stephanie Lin, Mateusz Litwin, Theresa Lopez, Ryan Lowe, Patricia Lue, Anna Makanju, Kim Malfacini, Sam Manning, Todor Markov, Yaniv Markovski, Bianca Martin, Katie Mayer, Andrew Mayne, Bob McGrew, Scott Mayer McKinney, Christine McLeavey, Paul McMillan, Jake McNeil, David Medina, Aalok Mehta, Jacob Menick, Luke Metz, Andrey Mishchenko, Pamela Mishkin, Vinnie Monaco, Evan Morikawa, Daniel Mossing, Tong Mu, Mira Murati, Oleg Murk, David Mély, Ashvin Nair, Reiichiro Nakano, Rajeev Nayak, Arvind Neelakantan, Richard Ngo, Hyeonwoo Noh, Long Ouyang, Cullen O’Keefe, Jakub Pachocki, Alex Paino, Joe Palermo, Ashley Pantuliano, Giambattista Parascandolo, Joel Parish, Emy Parparita, Alex Passos, Mikhail Pavlov, Andrew Peng, Adam Perelman, Filipe de Avila Belbute Peres, Michael Petrov, Henrique Ponde de Oliveira Pinto, Michael, Pokorny, Michelle Pokrass, Vitchyr H. Pong, Tolly Powell, Alethea Power, Boris Power, Elizabeth Proehl, Raul Puri, Alec Radford, Jack Rae, Aditya Ramesh, Cameron Raymond, Francis Real, Kendra Rimbach, Carl Ross, Bob Rotsted, Henri Roussez, Nick Ryder, Mario Saltarelli, Ted Sanders, Shibani Santurkar, Girish Sastry, Heather Schmidt, David Schnurr, John Schulman, Daniel Selsam, Kyla Sheppard, Toki Sherbakov, Jessica Shieh, Sarah Shoker, Pranav Shyam, Szymon Sidor, Eric Sigler, Maddie Simens, Jordan Sitkin, Katarina Slama, Ian Sohl, Benjamin Sokolowsky, Yang Song, Natalie Staudacher, Felipe Petroski Such, Natalie Summers, Ilya Sutskever, Jie Tang, Nikolas Tezak, Madeleine B. Thompson, Phil Tillet, Amin Tootoonchian, Elizabeth Tseng, Preston Tuggle, Nick Turley, Jerry Tworek, Juan Felipe Cerón Uribe, Andrea Valone, Arun Vijayvergiya, Chelsea Voss, Carroll Wainwright, Justin Jay Wang, Alvin Wang, Ben Wang, Jonathan Ward, Jason Wei, CJ Weinmann, Akila Welihinda, Peter Welinder, Jiayi Weng, Lilian Weng, Matt Wiethoff, Dave Willner, Clemens Winter, Samuel Wolrich, Hannah Wong, Lauren Workman, Sherwin Wu, Jeff Wu, Michael Wu, Kai Xiao, Tao Xu, Sarah Yoo, Kevin Yu, Qiming Yuan, Wojciech Zaremba, Rowan Zellers, Chong Zhang, Marvin Zhang, Shengjia Zhao, Tianhao Zheng, Juntang Zhuang, William Zhuk, and Barret Zoph. Gpt-4 technical report, 2024. 1, 2
- [25] Dustin Podell, Zion English, Kyle Lacey, Andreas Blattmann, Tim Dockhorn, Jonas Müller, Joe Penna, and Robin Rombach. Sd-xl: Improving latent diffusion models for high-resolution image synthesis, 2023. 1, 2
- [26] Rafael Rafailov, Archit Sharma, Eric Mitchell, Stefano Ermon, Christopher D. Manning, and Chelsea Finn. Direct preference optimization: Your language model is secretly a reward model, 2024. 1, 3
- [27] Robin Rombach, Andreas Blattmann, Dominik Lorenz, Patrick Esser, and Björn Ommer. High-resolution image synthesis with latent diffusion models, 2022. 1, 2
- [28] Chitwan Saharia, William Chan, Saurabh Saxena, Lala Li, Jay Whang, Emily Denton, Seyed Kamyar Seyed Ghasemipour, Burcu Karagol Ayan, S. Sara Mahdavi, Rapha Gontijo Lopes, Tim Salimans, Jonathan Ho, David J Fleet, and Mohammad Norouzi. Photorealistic text-to-image diffusion models with deep language understanding, 2022. 1, 2
- [29] Arne Schneuing, Charles Harris, Yuanqi Du, Kieran Didi, Arian Jamasb, Iliia Igashov, Weitao Du, Carla Gomes, Tom Blundell, Pietro Lio, Max Welling, Michael Bronstein, and Bruno Correia. Structure-based drug design with equivariant diffusion models, 2024. 1, 2
- [30] John Schulman, Filip Wolski, Prafulla Dhariwal, Alec Radford, and Oleg Klimov. Proximal policy optimization algorithms, 2017. 1
- [31] Jiaming Song, Chenlin Meng, and Stefano Ermon. Denoising diffusion implicit models, 2022. 2, 6
- [32] Haoyuan Sun, Bo Xia, Yongzhe Chang, and Xueqian Wang. Generalizing alignment paradigm of text-to-image generation with preferences through f-divergence minimization. *ArXiv*, abs/2409.09774, 2024. 8
- [33] Hugo Touvron, Louis Martin, Kevin Stone, Peter Albert, Amjad Almahairi, Yasmine Babaei, Nikolay Bashlykov, Soumya Batra, Prajjwal Bhargava, Shruti Bhosale, Dan Bikel, Lukas Blecher, Cristian Canton Ferrer, Moya Chen, Guillem Cucurull, David Esiobu, Jude Fernandes, Jeremy Fu, Wenyin Fu, Brian Fuller, Cynthia Gao, Vedanuj Goswami, Naman Goyal, Anthony Hartshorn,

- Saghar Hosseini, Rui Hou, Hakan Inan, Marcin Kardas, Viktor Kerkez, Madian Khabsa, Isabel Kloumann, Artem Korenev, Punit Singh Koura, Marie-Anne Lachaux, Thibaut Lavril, Jenya Lee, Diana Liskovich, Yinghai Lu, Yuning Mao, Xavier Martinet, Todor Mihaylov, Pushkar Mishra, Igor Molybog, Yixin Nie, Andrew Poulton, Jeremy Reizenstein, Rashi Rungta, Kalyan Saladi, Alan Schelten, Ruan Silva, Eric Michael Smith, Ranjan Subramanian, Xiaoqing Ellen Tan, Binh Tang, Ross Taylor, Adina Williams, Jian Xiang Kuan, Puxin Xu, Zheng Yan, Iliyan Zarov, Yuchen Zhang, Angela Fan, Melanie Kambadur, Sharan Narang, Aurelien Rodriguez, Robert Stojnic, Sergey Edunov, and Thomas Scialom. Llama 2: Open foundation and fine-tuned chat models, 2023. [2](#)
- [34] Bram Wallace, Meihua Dang, Rafael Rafailov, Linqi Zhou, Aaron Lou, Senthil Purushwalkam, Stefano Ermon, Caiming Xiong, Shafiq Joty, and Nikhil Naik. Diffusion model alignment using direct preference optimization, 2023. [1](#), [3](#), [6](#)
- [35] Zijie J. Wang, Evan Montoya, David Munechika, Haoyang Yang, Benjamin Hoover, and Duen Horng Chau. Large-scale prompt gallery dataset for text-to-image generative models. *arXiv:2210.14896 [cs]*, 2022. [6](#)
- [36] Xiaoshi Wu, Yiming Hao, Keqiang Sun, Yixiong Chen, Feng Zhu, Rui Zhao, and Hongsheng Li. Human preference score v2: A solid benchmark for evaluating human preferences of text-to-image synthesis, 2023. [1](#), [6](#)
- [37] Wei Xiong, Hanze Dong, Chenlu Ye, Ziqi Wang, Han Zhong, Heng Ji, Nan Jiang, and Tong Zhang. Iterative preference learning from human feedback: Bridging theory and practice for rlhf under kl-constraint, 2024. [1](#)
- [38] Shusheng Xu, Wei Fu, Jiaxuan Gao, Wenjie Ye, Weilin Liu, Zhiyu Mei, Guangju Wang, Chao Yu, and Yi Wu. Is dpo superior to ppo for llm alignment? a comprehensive study, 2024. [2](#), [4](#)
- [39] Kai Yang, Jian Tao, Jiafei Lyu, Chunjiang Ge, Jiabin Chen, Qimai Li, Weihang Shen, Xiaolong Zhu, and Xiu Li. Using human feedback to fine-tune diffusion models without any reward model, 2024. [1](#), [3](#), [4](#), [5](#)
- [40] Weizhe Yuan, Richard Yuanzhe Pang, Kyunghyun Cho, Xian Li, Sainbayar Sukhbaatar, Jing Xu, and Jason Weston. Self-rewarding language models, 2024. [1](#)
- [41] Junzi Zhang, Jongho Kim, Brendan O’Donoghue, and Stephen Boyd. Sample efficient reinforcement learning with reinforce, 2020. [1](#)